Stars and their variability observed from space
C. Neiner, W. W. Weiss, D. Baade, R. E. Griffin, C. C. Lovekin, A. F. J. Moffat (eds)

ASTEROSEISMOLOGY OF RAPIDLY ROTATING STARS WITH ACOUSTIC MODES

D. R. Reese[1]

Abstract.
Recent observations of mixed modes in red giants has revealed the shortcomings of current theory for explaining stellar rotation and angular momentum transport. Such shortcomings become more acute in the case of rapidly rotating stars, where the relevant physical processes such as baroclinicity are amplified. A series of recent stellar models based on 1D and 2D numerical approaches are starting to provide insights into these questions, but require observational constraints. Stellar pulsations potentially provide the tightest constraints on internal stellar structure but need to be identified correctly. The present contribution focusses on acoustic pulsations of rapidly rotating stars. After recalling the asymptotic behaviour of so-called island modes, the rotating counterparts to low-degree modes, it describes generalized rotational splittings and the insights they provide for the stellar rotation profile. It then describes recent efforts at interpreting observed pulsations, in particular searches for regular frequency patterns in different stars, and also multi-colour mode identification in β Pictoris using observations from various instruments, including the BRITE constellation.

Keywords: Stars: oscillations (including pulsations), rotation, interiors, evolution, fundamental parameters, stars: individual: 38 Eridani, β Pictoris, Rasalhague, Altair

1 Introduction

Many early-type main sequence stars rotate rapidly (*e.g.* Royer 2009). They include g-mode pulsating classes of stars, namely γ Dor stars and SPBs, as well as acoustic pulsators, namely δ Scuti and β Cep stars. Gravity-mode pulsators are described by Ouazzani (PAGE), but this contribution focusses on acoustic pulsators.

Currently, exquisite space photometry of pulsating stars has been, or will be, provided by the missions *MOST, CoRoT, Kepler* and $K2$ for a single photometric band, and by BRITE and PLATO for multiple colours. In parallel, the ground-based network SONG is starting to provide high-quality spectroscopic time-series for these stars. However, in the case of rapidly rotating acoustic pulsators, theoretical interpretations of asteroseismic data are lagging behind. There is a number of theoretical hurdles to overcome in modelling such stars, such as centrifugal deformation and baroclinicity. Furthermore, mode identification, i.e., matching observed pulsations with theoretically calculated modes, is very challenging. Nonetheless, gaining a better understanding of these stars would provide insights into baroclinic flows, transport processes of angular momentum and chemical species, and the effects of these phenomena on stellar lifetime and chemical yields. It would lead to a better modelling of the precursors to supernovæ and γ-ray bursts. This contribution will therefore describe recent insights in the theoretical modelling of acoustic pulsations of such stars, (Sect. 2) and also some of the latest asteroseismic investigations that have been carried out (Sect. 3).

2 Rotation and pulsations

Acoustic modes are high-frequencies modes for which the restoring force is pressure. They are especially affected by the centrifugal force. Those effects can be characterised by the ratio of the stellar flattening $\epsilon = 1 - R_{\rm p}/R_{\rm eq} \propto \Omega^2$, where $R_{\rm p}$ and $R_{\rm eq}$ are the polar and equatorial radii, and Ω the rotation rate, to the mode wavelength $\lambda \propto \omega^{-1}$, where ω is the pulsation frequency. Accordingly, high-requency modes are affected more quickly than low-frequency modes for increasing rotation rates (*e.g.* Reese et al. 2006).

At high rotation rates, different classes of acoustic pulsation modes appear, as shown by ray dynamics (Lignières & Georgeot 2008, 2009), which are characterised by distinct mode geometries and frequency organisation in the pulsation spectrum. These classes include island modes, chaotic modes and whispering gallery modes, and are the rotating counterparts to modes with low, intermediate, and high values of $\ell - |m|$. Mirouh et al. (2019) recently put together a convolution neural network to classify theoretically calculated modes automatically according to these different classes, thus avoiding laborious manual classification.

[1] LESIA, Observatoire de Paris, Université PSL, CNRS, Sorbonne Université, Université de Paris, 5 place Jules Janssen, 92195 Meudon, France

2.1 Island modes

Of these different classes, island modes are probably the most interesting, as they are the most visible of the regular modes (Lignières & Georgeot 2009; Reese et al. 2013). They are characterised by the quantum numbers $\tilde{n}$, the number of nodal lines which are perpendicular to the underlying periodic orbit, $\tilde{\ell}$, the number of nodal lines parallel to the orbit, and m, the azimuthal order. By using these quantum numbers, one can obtain an asymptotic expression for their frequencies in an inertial frame (*e.g.* Reese et al. 2009):

$$\omega \simeq \Delta_{\tilde{n}}\tilde{n} + \Delta_{\tilde{\ell}}\tilde{\ell} + \frac{\Delta_{\tilde{m}} m^2}{\tilde{n}^2} - m\Omega + \tilde{\alpha} \tag{2.1}$$

The quantity $\Delta_{\tilde{n}}$ is deduced from the acoustic travel time along the underlying orbit (Lignières & Georgeot 2008, 2009), and is roughly proportional to $\sqrt{\bar{\rho}}$, where $\bar{\rho}$ is the mean density (Reese et al. 2008; García Hernández et al. 2015). A semi-analytical formula for $\Delta_{\tilde{\ell}}$ has also been obtained by Pasek et al. (2011, 2012).

An important question is whether it is possible to probe the rotation profile using island modes. In order to answer it, we can already investigate the forward problem, i.e., how do different rotation profiles affect the pulsation frequencies. Reese et al. (2009, submitted) derived a formula that relates the generalised rotational splittings, defined as the splitting between a prograde mode and its retrograde counterpart, to weighted integrals of the rotation profile, where the weighting is mode-dependant:

$$\frac{\omega_{-\mathrm{m}} - \omega_{\mathrm{m}}}{2m} \simeq \frac{\Omega_{\mathrm{m}}^{\mathrm{eff}} + \Omega_{-\mathrm{m}}^{\mathrm{eff}}}{2} + \frac{\mathcal{C}_{\mathrm{m}} + \mathcal{C}_{-\mathrm{m}}}{2} \tag{2.2}$$

with

$$\Omega_{\mathrm{eff}} = \frac{\int_V \Omega \rho_o \|\vec{\xi}\|^2 dV}{\int_V \rho_o \|\vec{\xi}\|^2 dV} \tag{2.3}$$

$$\mathcal{C} = \frac{i}{m} \frac{\int_V \rho_o \vec{\Omega} \cdot \left(\vec{\xi}^* \times \vec{\xi}\right) dV}{\int_V \rho_o \|\vec{\xi}\|^2 dV}, \tag{2.4}$$

where $-m$ corresponds to prograde modes, ρ_o is the equilibrium density profile, and $\vec{\xi}$ the Lagrangian displacement. Applying this formula to the profiles shown in the left part of Fig. 1 using $\tilde{\ell} = 0$ modes leads to the splittings in the right panel of the figure. A clear distinction can be seen between profiles with a radial gradient but only a small horizontal gradient (ESTER and Shellular) and those with a stronger horizontal gradient (Cylindrical and Conical). Also shown in the right panel are the true splittings, which should be compared with those deduced for the ESTER profile using the above formula (thus giving an idea of the accuracy of the formula).

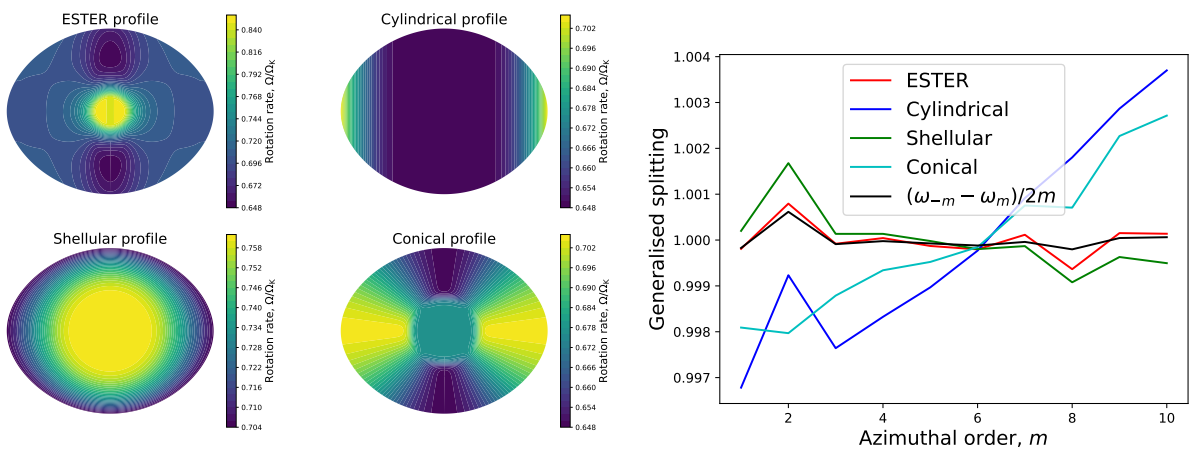

Fig. 1. Four different rotation profiles (**left**) and the resultant generalised rotational splittings for a set of $\tilde{\ell} = 0$ modes with m ranging from 1 to 10 using Eq. (2.2) (**right**). The true splittings are also shown in black in the right panel.

2.2 Chaotic modes

Chaotic modes are characterised by a chaotic mode structure (as expected, based on the relevant ray trajectories) and a statistical distribution of pulsation frequencies rather than an asymptotic formula. Nonetheless, Evano et al. (2019a,b) recently showed that these modes also display partial regularities. As revealed through peaks in the autocorrelation functions of their pulsation spectra, a characteristic spacing close to the large frequency separation is present – as can be seen in the echelle diagram shown in the left panel of Fig. 2. The modes associated with a given ridge in the echelle diagram also have a similar geometric structure, as illustrated in the right panel of Fig. 2.

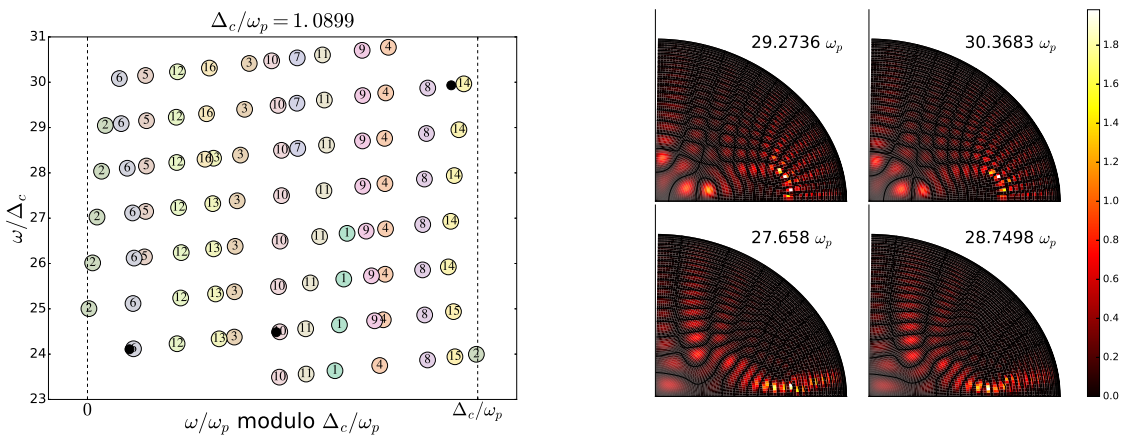

Fig. 2. (**Left**:) Echelle diagram with chaotic modes. The colours and numbers highlight different ridges composed of modes with a similar geometric structure. (**Right**:) Meridional cross sections of consecutive chaotic modes from series 8 (upper row) and 3 (lower row). From Evano et al. (2019b), reproduced with permission ©ESO.

Such regularities are not expected in the context of quantum chaos theory, i.e., the theory which provides the link between eigenvalue spectra and chaotic ray trajectories. As argued in Evano et al. (2019a,b), the cause behind this behaviour is the strong stratification in sound velocity in the radial direction which leads to a fairly regular structure in that direction, even if the latitudinal structure is chaotic.

3 Interpreting observations

Various approaches have been used to interpret the acoustic pulsations of rapidly rotating stars. They include the search for frequency patterns, multi-colour mode identification, and combining asteroseismic constraints with other constraints, in particular those from interferometry.

3.1 Frequency patterns

As was shown in various theoretical calculations (*e.g.* Lignières et al. 2006; Reese et al. 2008), the large frequency separation, $\Delta\nu$, continues to exist at high rotation rates and to scale with the mean density. Accordingly, García Hernández et al. (2013, 2015); García Hernández et al. (2017) have identified $\Delta\nu$ through Fourier transforms of the pulsation spectra and used it to constrain $\bar{\rho}$ and $\log(g)$, the surface gravity, in δ Scuti stars. Michel et al. (2017) stacked the pulsation spectra from multiple main-sequence δ Scuti stars observed by *CoRoT*, thus revealing the presence of similar frequency spacings in these stars. Bowman & Kurtz (2018) repeated the same exercise for *Kepler* stars but their results were less clear.

Once a recurrent frequency separation has been found, it is possible to construct echelle diagrams with the pulsation frequencies. That has been done by García Hernández et al. (2013); Paparó et al. (2016a,b) for *CoRoT* stars, and more recently by Bedding et al. (2020) for TESS stars. Ridges appear in the echelle diagrams and have been interpreted as axisymmetric $\ell = 0$ and 1 modes in Bedding et al. (2020). Indeed, up to rapid rotation rates, the normalised frequencies for axisymmetric $\ell = 0$ and 1 modes vary little, apart from the occasional avoided crossing, as illustrated in Fig. 3.

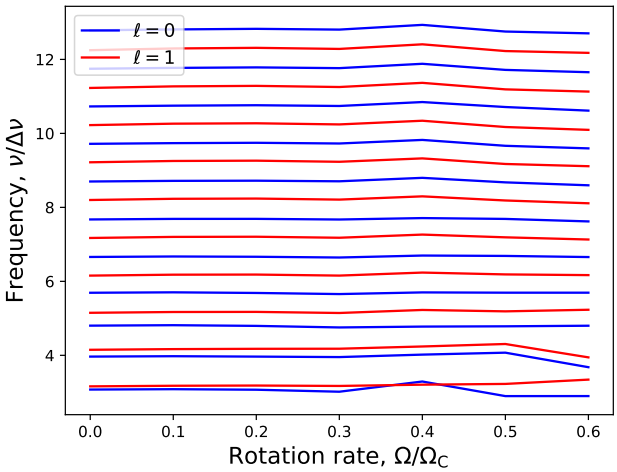

Fig. 3. Axisymmetric $\ell = 0$ and 1 mode frequencies, normalised by the large separation for $1.8\,M_\odot$ ZAMS models ranging from $0 - 0.6\Omega_C$ calculated with the Self-Consistent Field (SCF) method (Jackson et al. 2005; MacGregor et al. 2007). Ω_C is the critical rotation rate and is very close to the Keplerian break-up rotation rate (see Table 1 of Reese et al. 2013).

3.2 Multi-colour mode identification

For a given pulsation mode, the amplitude ratios and phase differences between different photometric bands depends only on its geometric characteristics. Hence, measuring these quantities provides constraints on the identification of the observed modes. Although quite popular for slowly rotating stars, this method has not been applied extensively to rapid rotators; in fact, in the rotating case, amplitude ratios depend on the inclination of the star and the azimuthal order (Daszyńska-Daszkiewicz et al. 2002; Townsend 2003), thus complicating the identification process.

Recently, Paparó et al. (2018) studied 38 Eri, a δ Scuti star with $v \sin i = 98\,\mathrm{km\ s^{-1}}$, using ground-based observations in multiple photometric bands from the Strömgren and Johnson systems, and also space photometry data from the MOST satellite, and found 18 pulsation frequencies corresponding to low order p and g modes. They went on to carry out mode identification using amplitude ratios (without including the effects of rotation) and what appears to be g-mode rotational splittings. However, the two approaches produced conflicting results, thus pointing to a need for further analysis including full 2D-mode visibility calculations when interpreting the results.

More recently, Zwintz et al. (2019) studied β Pic, a δ Scuti star rotating at $v \sin i = 124 \pm 3, \mathrm{km\ s^{-1}}$ and with a disk and an exoplanet (Lagrange et al. 2010), and found 15 pulsation frequencies in 2 to 5 photometric bands from multiple instruments, namely the BRITE blue and red satellites, bRing*, SMEI†, and ASTEP. They carried out a detailed asteroseismic analysis using $1.8\,M_\odot$ ZAMS models with rotation rates from $0-0.6\,\Omega_C$ based on the Self-Consistent Field (SCF) method (Jackson et al. 2005; MacGregor et al. 2007). Multi-colour mode visibility calculations including an approximate treatment of non-adiabatic effects were carried out following Reese et al. (2013, 2017b). An MCMC fit to the amplitude ratios and pulsation frequencies, including various classic constraints, was performed, and led to a variety of solutions depending on the weight factors for the different constraints. Figure 4 shows a comparison between observed and theoretical amplitude ratios and frequencies, for a near-equator-on configuration of the star (which is what would be expected if the star were aligned with the disk and exoplanet orbit). It illustrates the challenges in reproducing the observations and the need for developing theoretical predictions further.

3.3 Combining asteroseismology and interferometry

When stars rotate rapidly, it can be particularly interesting to combine the constraints from interferometry with those from asteroseismology. Indeed, interferometry provides constraints on the stellar radius (when combined with the parallax), the rotation rate (by measuring the amount of centrifugal deformation), and inclination (thanks to gravity darkening). Those in turn narrow down the possibilities when searching for models which reproduce the asteroseismic constraints.

*The β Pictoris b Ring project.
†Solar Mass Ejection Image

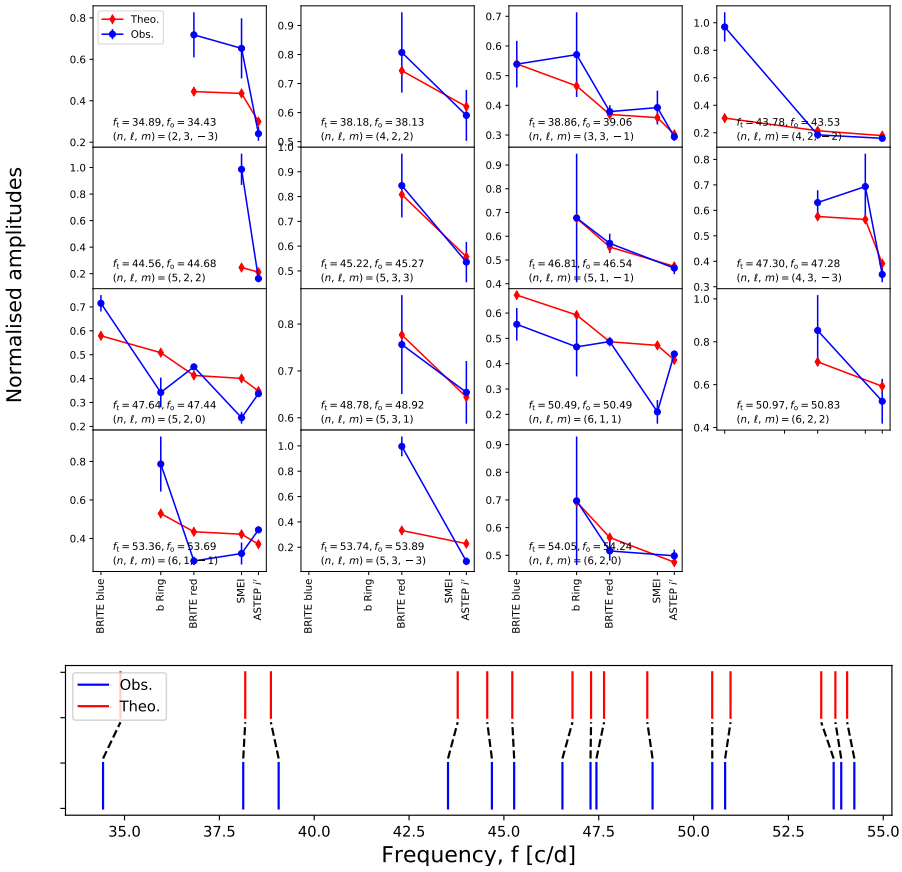

Fig. 4. A comparison between observed and theoretical amplitude ratios (**upper panel**) and frequencies (**lower panel**) for β Pic. From Zwintz et al. (2019).

The δ Scuti star α Ophiuchi ('Rasalhague') has been observed interferometrically, and led to a precise determination of its inclination, polar and equatorial radii (Zhao et al. 2009). 57 pulsation frequencies have been detected, thanks to MOST photometry (Monnier et al. 2010). Deupree (2011); Deupree et al. (2012) carried out asteroseismic studies of this star using a 2D approach. However, a precise mode identification remained elusive owing to the multitude of theoretical pulsation modes which could potentially match the observed frequencies. More recently, Mirouh et al. (2017) studied this star using 2D ESTER models (Espinosa Lara & Rieutord 2013; Rieutord et al. 2016) which fit the interferometric constraints. They carried out an asteroseismic fit taking into account mode visibilities and excitation, and using the non-adiabatic version of the 2D pulsation code TOP (Reese et al. 2006, 2017a). The results were not conclusive, owing to the lack of excited island modes; that points towards limitations in the models and/or the pulsation calculations.

More recently still, Bouchaud et al. (submitted) carried out an in-depth study of the star α Aquilae ('Altair'). As a first step, they fitted the interferometric constraints from the PIONIER and GRAVITY instruments at the VLTI and also some spectroscopic constraints, using Roche Models with the gravity darkening prescription from Espinosa Lara & Rieutord (2011) and full 2D ESTER models. That led to well-constrained values for the equatorial radius, the rotation rate, the inclination and position angle. However, a degeneracy appeared between the mass, the metallicity, the envelope and the core hydrogen content. Using the pulsation frequencies obtained with WIRE (Buzasi et al. 2005), and assuming they were the rotating counterparts to $\ell = 0$ and 1 modes, they were able to constrain the mass to $1.86 \pm 0.03\, M_{\odot}$, and thence narrow down the other parameters as well, thus showing that Altair is close to the ZAMS. The theoretical mode visibilities were also shown to behave qualitatively in a manner similar to the observed amplitudes, as illustrated in Fig. 5.

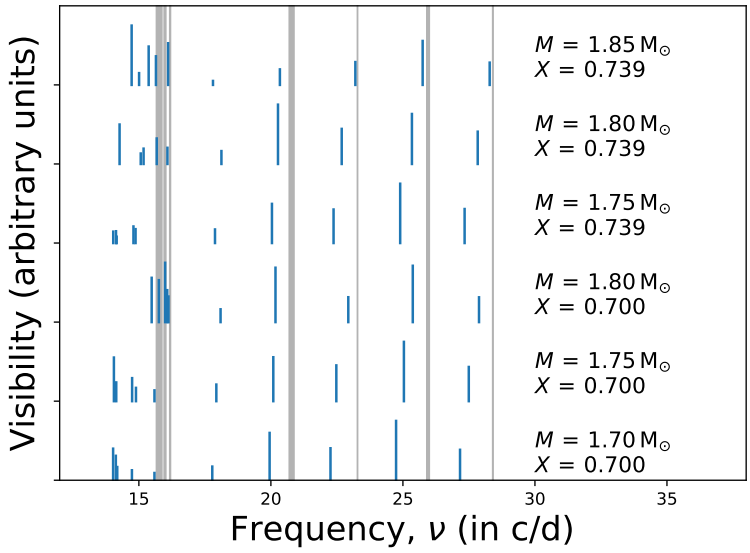

Fig. 5. A comparison between observed and theoretical pulsation spectra for Altair. The vertical grey lines correspond to observed pulsations; their thicknesses indicate the amplitudes. The blue segments correspond to theoretical modes from six ESTER models (1 per row). Their lengths correspond to mode visibilities. From Bouchaud et al. (submitted).

4 Conclusions

As can be seen, much progress has been made both in terms of theoretical developments for acoustic modes in rapidly rotating stars and in terms of interpreting observations. One can, for instance, cite the unexpected regularity in the pulsation spectra of chaotic modes, the discovery of frequency patterns in a number of δ Scuti stars, or the finding of plausible identifications for individual modes. This opens up various prospects, such as the possibility of constraining global stellar parameters for these stars, probing their internal rotation profiles, or providing insights into the different transport processes occurring in them as a result of rotation.

DRR gratefully acknowledges support of the French Agence Nationale de la Recherche (ANR) for the ESRR project under grant ANR-16-CE31-0007, and financial support from the Programme National de Physique Stellaire (PNPS) of the CNRS/INSU co-funded by the CEA and the CNES. DRR benefited from the hospitality of ISSI as part of the SoFAR team early in 2018 and 2019.

References

Bedding, T. R., Murphy, S. J., Hey, D. R., et al. 2020

Bouchaud, K., Domiciano de Souza, A., Rieutord, M., Reese, D. R., & Kervella, P. submitted, A&A

Bowman, D. M. & Kurtz, D. W. 2018, MNRAS, 476, 3169

Buzasi, D. L., Bruntt, H., Bedding, T. R., et al. 2005, ApJ, 619, 1072

Daszyńska-Daszkiewicz, J., Dziembowski, W. A., Pamyatnykh, A. A., & Goupil, M.-J. 2002, A&A, 392, 151

Deupree, R. G. 2011, ApJ, 742, 9

Deupree, R. G., Castañeda, D., Peña, F. o., & Short, C. I. 2012, ApJ, 753, 20

Espinosa Lara, F. & Rieutord, M. 2011, A&A, 533, A43

Espinosa Lara, F. & Rieutord, M. 2013, A&A, 552, A35

Evano, B., Georgeot, B., & Lignières, F. 2019a, EPL (Europhysics Letters), 125, 49002

Evano, B., Lignières, F., & Georgeot, B. 2019b, A&A, 631, A140

García Hernández, A., Martín-Ruiz, S., Monteiro, M. J. P. F. G., et al. 2015, ApJ Letter, 811, L29

García Hernández, A., Moya, A., Michel, E., et al. 2013, A&A, 559, A63

García Hernández, A., Suárez, J. C., Moya, A., et al. 2017, MNRAS, 471, L140

Jackson, S., MacGregor, K. B., & Skumanich, A. 2005, ApJS, 156, 245

Lagrange, A. M., Bonnefoy, M., Chauvin, G., et al. 2010, Science, 329, 57

Lignières, F. & Georgeot, B. 2008, Phys. Rev. E, 78, 016215

Lignières, F. & Georgeot, B. 2009, A&A, 500, 1173

Lignières, F., Rieutord, M., & Reese, D. 2006, A&A, 455, 607

MacGregor, K. B., Jackson, S., Skumanich, A., & Metcalfe, T. S. 2007, ApJ, 663, 560

Michel, E., Dupret, M.-A., Reese, D., et al. 2017, in EPJ Web of Conferences, Vol. 160, EPJ Web of Conferences, 03001

Mirouh, G. M., Angelou, G. C., Reese, D. R., & Costa, G. 2019, MNRAS, 483, L28

Mirouh, G. M., Reese, D. R., Rieutord, M., & Ballot, J. 2017, in SF2A-2017: Proceedings of the Annual meeting of the French Society of Astronomy and Astrophysics, Di

Monnier, J. D., Townsend, R. H. D., Che, X., et al. 2010, ApJ, 725, 1192

Paparó, M., Benkő, J. M., Hareter, M., & Guzik, J. A. 2016a, ApJ, 822, 100

Paparó, M., Benkő, J. M., Hareter, M., & Guzik, J. A. 2016b, ApJS, 224, 41

Paparó, M., Kolláth, Z., Shobbrook, R. R., et al. 2018, MNRAS, 477, 4362

Pasek, M., Georgeot, B., Lignières, F., & Reese, D. R. 2011, Physical Review Letters, 107, 121101

Pasek, M., Lignières, F., Georgeot, B., & Reese, D. R. 2012, A&A, 546, A11

Reese, D., Lignières, F., & Rieutord, M. 2006, A&A, 455, 621

Reese, D., Lignières, F., & Rieutord, M. 2008, A&A, 481, 449

Reese, D. R., Dupret, M.-A., & Rieutord, M. 2017a, in EPJ Web of Conferences, Vol. 160, EPJ Web of Conferences, 02007

Reese, D. R., Lignières, F., Ballot, J., et al. 2017b, A&A, 601, A130

Reese, D. R., MacGregor, K. B., Jackson, S., Skumanich, A., & Metcalfe, T. S. 2009, A&A, 506, 189

Reese, D. R., Mirouh, G. M., Espinosa Lara, F., Rieutord, M., & Putigny, B. submitted, A&A

Reese, D. R., Prat, V., Barban, C., van 't Veer-Menneret, C., & MacGregor, K. B. 2013, A&A, 550, A77

Rieutord, M., Espinosa Lara, F., & Putigny, B. 2016, Journal of Computational Physics, 318, 277

Royer, F. 2009, On the Rotation of A-Type Stars, Vol. 765 (Berlin: Springer), 207–230

Townsend, R. H. D. 2003, MNRAS, 343, 125

Zhao, M., Monnier, J. D., Pedretti, E., et al. 2009, ApJ, 701, 209

Zwintz, K., Reese, D. R., Neiner, C., et al. 2019, A&A, 627, A28